Effects of Water on the Preparation, Morphology, and Properties of Polyimide/Silica Nanocomposite Films Prepared by Sol–Gel Process

Lizhong Jiang, Wencai Wang, Xiaowei Wei, Dezhen Wu, Riguang Jin

State Key Laboratory of Chemical Resource Engineering, Beijing University of Chemical Technology, Beijing 100029, People's Republic of China

Received 14 December 2005; accepted 23 October 2006
DOI 10.1002/app.25692
Published online in Wiley InterScience (www.interscience.wiley.com).

ABSTRACT: Polyimide/silica (PI/SiO_2) nanocomposite films with 10 wt % of silica content were prepared by sol–gel process under the conditions with and without additional water. The presence of additional water has great effect on the silica particle size and thus on the properties of the prepared PI/SiO_2 films. The results indicated that with additional water, the silica particles formed before the imidization of poly(amic acid) (PAA) and aggregated with the increasing of temperature and degree of the proceeding imidization process. For the nonaqueous process, the hydrolysis condensation reaction of tetraethoxysilane (TEOS) did not occur until the imidization of PAA took place, and no silica particles were found in the unimidized PAA films. The hydrolysis–condensation reaction of TEOS was initiated simultaneously by the trace water released from the imidization reaction, the self-catalysis mechanism of the approach provide a means of achieving uniformly dispersed silica particles formed in the PI matrix with particle size in the range of 30–70 nm. © 2007 Wiley Periodicals, Inc. J Appl Polym Sci 104: 1579–1586, 2007

Key words: nanocomposite; polyimide; silica; morphology

INTRODUCTION

In recent years, increased attention has been paid to preparing organic–inorganic nanocomposites that combine the advantages of organic components (flexibility, low dielectric constant, and processibility) and inorganic components (rigidity, strength, durability, and thermal stability).[1–8] To improve the thermal stability and mechanical strength of polyimides, polyimide/silica (PI/SiO_2) composites have been under extensive study. A variety of approaches to obtain PI/SiO_2 nanocomposites have been attempted. Among them, the sol–gel process is the most common method, which can form inorganic frameworks under mild condition.[9–12] The sol–gel process consists of a two-step reaction, as shown in Figure 1. The inorganic alkoxides are hydrolyzed to produce hydroxyl groups, followed by condensation of the hydrolysis products to form a three-dimensional silica network. Actually, the hydrolysis and condensation reactions occur simultaneously.[13] A lot of factors influence the structure of the silica network produced by the hydrolysis and condensation reactions in the sol–gel process, including the alkoxide structure, pH, solvent, catalyst, temperature, and pressure.[14] Generally, acid catalyzed systems form more linear structures, whereas base catalyzed systems favor the formation of highly branched clusters.[14] Altering the reaction variables will lead to different sol morphologies and final gel structure. Such studies fall into an extensive field of research known as sol–gel chemistry.

Most of the PI/SiO_2 nanocomposites are prepared by a three-step route: poly(amic acid) (PAA) is first synthesized, and then hydrolyzed tetraethoxysilane (TEOS) or the mixtures of H_2O and TEOS is added to form a homogeneous mixture with PAA; finally, the mixtures are heated gradually to imidize the PAA to PI and so obtain the PI/silica nanocomposites.[15] However, it was found that phase separation occurred at higher silica content, and mechanical strength of the resulting films had decreased, relative to those of the pristine PIs.[16] As a result, this will lead the PI/silica nanocomposites to be unpractical because of its high brittleness. To achieve PI/silica nanocomposites with good properties, compatibility of the PI and silica phases is a critical factor to be considered. Generally, compatibility improvement can be achieved through the improvement of the interaction between the two phases and by the reduction in the silica particle size. Various methods have been developed to enhance the compatibility of the organic and inorganic phase in this field.[17–22] To the best of our knowledge, although

Correspondence to: D. Wu (wdz@mail.buct.edu.cn).
Contract grant sponsor: National Natural Science Foundation of China; contract grant number: 50573007.
Contract grant sponsor: Ministry of State Science and Technology.

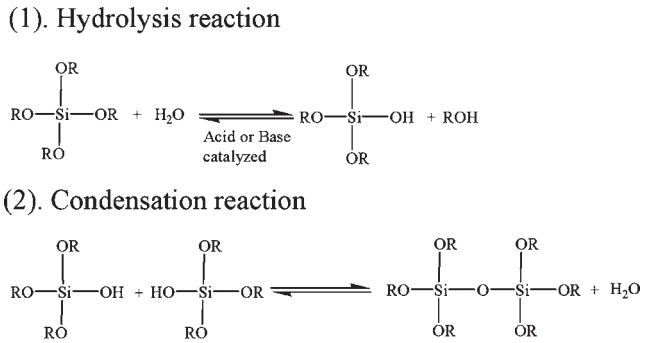

Figure 1 The hydrolysis and condensation reactions of the sol–gel process.

different approaches and factors have been widely studied, the effects of additional water in the sol–gel process on the generation and growth of silica particles is yet to be explored in detail.

In the present work, PI/SiO_2 nanocomposite films were prepared from pyromellitic dianhydride and 4,4′-oxydianiline (PMDA–ODA) and TEOS with different molar ratios of additional water. The imidization degree and molar ratios of additional water on the structures and morphologies of the obtained PI/Silica nanocomposites were investigated by Fourier-transformed infrared (FTIR) and transmission electron microscopy (TEM). The mechanical and thermal properties of PI/SiO_2 nanocomposite films were also studied by thermal gravimetric analyzer (TGA) and mechanical property measurements.

EXPERIMENTAL

Materials

PMDA and ODA were received from Shanghai Research Institute of Synthetic Resins, China, and were used after dehydration. *N*,*N*-dimethylacetamide (DMAc) and TEOS were purchased from Tianjin Fu Chen Chemicals Reagent, and were used as received.

Preparation of PI/SiO_2 nanocomposite films

In a 250 mL, three-necked round-bottomed flask fitted with a mechanical stirrer, 3.661 g (0.0183 mol) of ODA were dissolved in 60 mL of DMAc. An equimolar amount of dianhydride (PMDA) powder (4.030 g) was then introduced into the solution step wisely. The reaction mixture was stirred under nitrogen for over 12 h to make a PAA solution. Subsequently, certain amounts of TEOS and distilled water were added to the PAA solution and the mixture was further stirred for 6 h. The calculated content of SiO_2 in the nanocomposite films was 10 wt %, and the molar ratio of distilled water to TEOS was 16 : 1, 8 : 1, 4 : 1, 2 : 1, 1 : 1, and 0 : 1 respectively. The mixture was cast subsequently onto precleaned quartz wafers and heated gradually in an air-circulating oven with the curing procedure: 80°C for 1 h, 120°C for 1 h, 180°C for 1 h, 250°C for 1 h, and 300°C for 4 h. The films were allowed to cool down gradually to room temperature over a period of 6 h. Thermal curing gives PI/SiO_2 nanocomposite films in 25–35 μm in thickness and it was retrieved from the wafer by immersing the film in water for a few minutes.

Characterization

The FTIR spectra were recorded under ambient conditions on a Nexus 670 spectrometer with attenuated total reflection (ATR) accessory. Typically, 16 scans with a resolution of 8 cm^{-1} were accumulated to obtain the spectrum. TEM images were recorded on a HITACHI H-800 TEM transmission electron microscope at an accelerating voltage of 100 kV. The TEM samples were prepared using the Reichert Sung Ultracut E ultramicrotome at a temperature of −40°C. Thermal properties of PI/SiO_2 films were examined using dynamic thermal gravimetric analysis (TGA). Scans were run at a heating rate of 10–800°C/min in a flowing nitrogen atmosphere. The films were cut into strips of 4 mm × 25 mm in size to measure the mechanical properties of films with an Instron-1185 system at room temperature. All measurements were carried out at a cross-head speed of 10 mm/min. Each tensile strength reported was the average of at least five sample measurements.

RESULTS AND DISCUSSION

Characterization of the PI/SiO_2 nanocomposites by FTIR-ATR imidization degree

To study the effect of the imidization process of PAA to PI on the formation of the inorganic phase, the imidization degree, ID, is analyzed semiquantitatively by monitoring the absorption band at 1380 cm^{-1} for the imide group in the FTIR spectrum, as a function of temperature. Normalization of the peak's height to

compensate for the thickness variation was accomplished by ratioing against an internal reference band (the aromatic ring absorption at 1500 cm^{-1}), which was found to be constant with the chemical modifications occurring upon imidization. The ID at temperature T is evaluated as eq. (1):[23]

$$\mathrm{ID}(T) = \frac{A_T(1380)/A_T(1500)}{A_F(1380)/A_F(1500)} \quad (1)$$

where $A_T(1380)$ and $A_F(1380)$ are the absorbance bands at 1380 cm^{-1} at temperature T and for a completely imidized PI, respectively. $A_T(1500)$ and $A_F(1500)$ are the absorbance band at 1500 cm^{-1} at temperature T and for a completely imidized PI, respectively.

The FTIR–ATR spectra of the PI/silica films collected at different temperatures during the thermal curing process are shown in Figure 2. Compare the FTIR spectrum in Figure 2(a) with those in Figure 2(b–h); the conversion of PAA to PI could be elucidated by the decrease of the carbolic acid absorption at 3400 cm^{-1}(not shown) and the amide carbonyl absorption at 1650 cm^{-1}, the absorption bands at 1543 cm^{-1} for the characteristic peak of PAA, and the appearance of imide carbonyl absorption at 1780, 1717, 1380, and 725 cm^{-1}. With the increase of imidization temperature, the peak intensity of the characteristic absorption of imide group increases, which indicated the increase in imidization degree. On the other hand, however, the characteristic absorption of PAA disappeared gradually. These phenomena can qualitatively illustrate that the imidization process is gradually complete with increasing temperature.

Figure 3 shows the degree of imidization estimated semiquantitatively from the FTIR–ATR spectroscopic data, according to eq. (1). It can be observed that the imidization degree increased with the increase of temperature, and it approaches an asymptotic value at 300°C. This result shows that the PAA in the nanocomposite films were completely converted to PI.

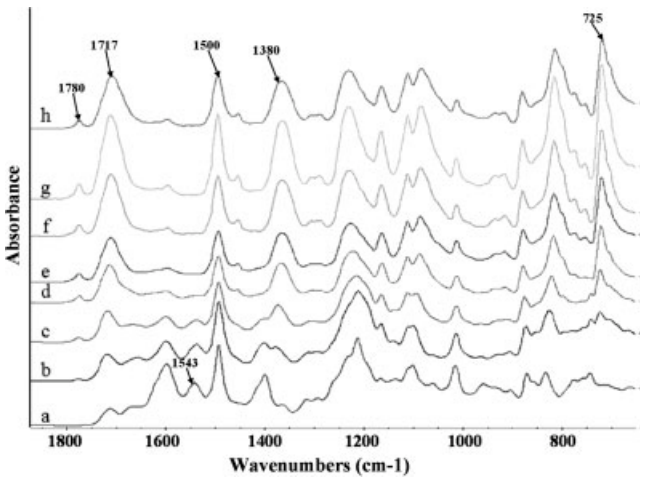

Figure 2 FTIR spectra of films collected at temperatures of: (a) 20°C, (b) 80°C, (c) 120°C, (d) 160°C, (e) 200°C, (f) 250°C, (g) 300°C, (h) 360°C.

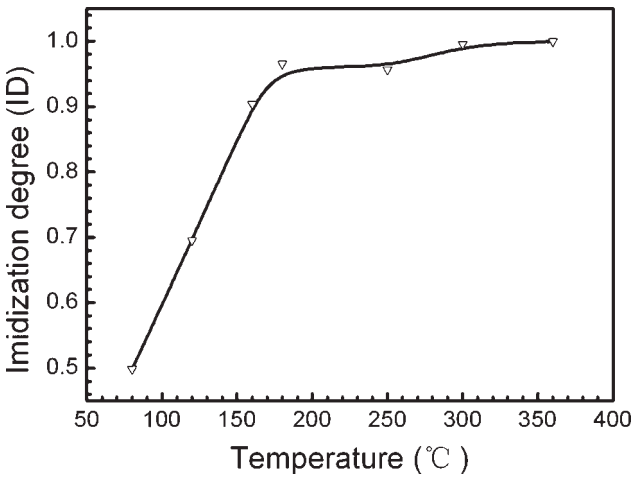

Figure 3 Imidization degree (ID) as a function of temperature for the thermal curing process.

Effect of additional water on the chemical structures of PI/SiO_2 nanocomposites

The sol–gel processes are affected by many controllable synthetic parameters, such as structure and concentration of reactants, solvent, catalysis, as well as reaction temperature, and the rate of removal of byproducts and solvent. From Figure 1, we can see that water plays an important role in the sol–gel process: the water is utilized in the hydrolysis process and generated in the condensation reaction. Generally, water is necessary for the reactions in the sol–gel process. The amount of water in the reaction could have an effect on the reaction rate of sol–gel process, and thus on the morphology of the PI/SiO_2 nanocomposites, such as the size and distribution of the silica particles in the PI matrix. It is well known that there is trace water released during the process of imidization of PAA to PI. The trace water can initiate the hydrolysis–condensation reaction of silica precursor. In this case, the trace water is *in situ* generated from the cycloimidization of PAA and simultaneously initiated the sol–gel process, and the silica particles generated and grew synchronically.

FTIR was used to evaluate the changes in the chemical structure of the PI/SiO_2 nanocomposites and the formation and growth of silica particles in the nanocomposite films. The FTIR absorbance spectra of the PI/SiO_2 nanocomposite films obtained by the sol–gel process with and without additional water at 20°C

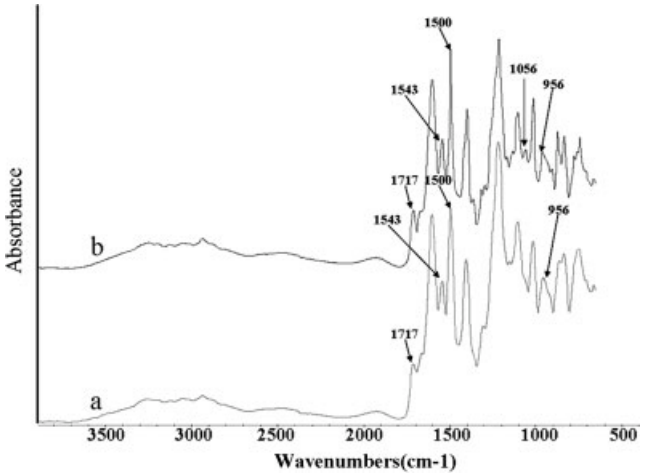

Figure 4 FTIR spectra of films obtained at 20°C: (a) with additional water (molar ratio of additional water to TEOS is 4 : 1) and (b) by a nonaqueous process.

are shown respectively, in Figure 4. Both of the films have the characteristic absorption bands at 2900–3200 cm^{-1} (υ_{-COOH} and υ_{N-H}), 1717 cm^{-1}($\upsilon_{C=O}$), 1543 cm^{-1} (δ_{N-H}), and 956 cm^{-1}($\upsilon_{Si-O-Et}$),[24] and no characteristic bands of imide group at 1780($\upsilon_{C=O}$), and 1380(υ_{C-N}), and 725 cm^{-1}($\delta_{C=O}$) was found. This result indicates that the imidization of PAA to PI did not occur. Comparing the FTIR spectrum in Figure 4(a) with that of Figure 4(b), it can be seen that an absorption band at 1056 cm^{-1} emerged, which is evidence for formation of Si—O—Si bonds. The result suggests that the hydrolysis–condensation reaction of TEOS occurred before imidization of PAA to PI because of the presence of additional water in the process, and the imidization reaction did not occur in the film without additional water.

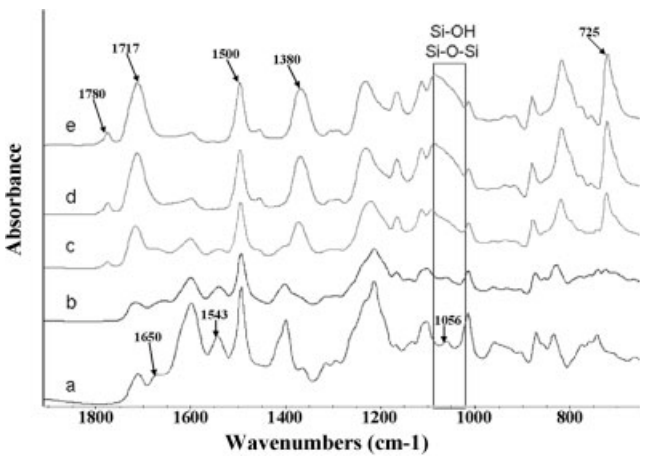

Figure 5 FTIR spectra of the nanocomposite film with 10 wt % silica content via sol–gel process with additional water (molar ratio of additional water to TEOS is 4 : 1) at temperatures of: (a) 20°C, (b) 80°C, (c) 120°C, (d) 160°C, (e) 200°C.

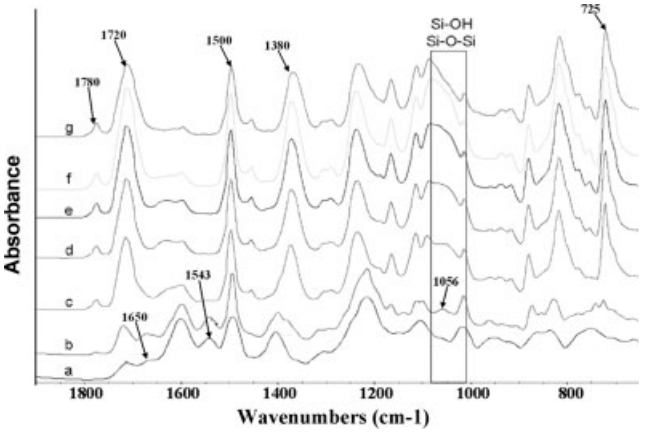

Figure 6 FTIR spectra of the nanocomposite film with 10 wt % silica content via sol–gel process without additional water at temperatures of: (a) 20°C, (b) 80°C, (c) 120°C, (d) 160°C, (e) 200°C, (f) 250°C, (g) 300°C.

Figures 5 and 6 show the FTIR spectra of the nanocomposite films obtained with and without additional water at different temperatures. It can bee seen that with increasing temperature, the characteristic absorption of TEOS at 956 cm^{-1} disappeared gradually, while the absorption band at 1000–1100 cm^{-1} appeared, indicating the presence of silica. The results confirm that the hydrolysis of TEOS gradually completed and the silica network generated. In addition, as shown in Figure 6, the characteristic absorption of silica was not found before the imidization process started. When the imidization reaction starts, the absorption bands appeared with the increase of the imidization degree, the intensity of the absorption bands increase and becomes broader. But these phenomena cannot be observed in Figure 5. It can be explained that the trace water release from the imidization of PAA to PI initiated the hydrolysis–condensation of TEOS to form silica particles. It will be further confirmed by the TEM results in the following part.

TEM morphology of the PI/SiO_2 nanocomposites

To investigate the distribution of silica particles and microphase separation in the PI matrix, the morphology of the nanocomposite films was investigated by TEM. Figure 7 shows the TEM images of PI/SiO_2 nanocomposites with 10 wt % content of silica by a nonaqueous process [Fig. 7(a)] and at different molar ratios of additional water to TEOS: (b) 1 : 1, (c) 2 : 1, (d) 4 : 1, (e) 8 : 1 and (f) 16 : 1, respectively. The mean size of silica particles assessed from the micrographs was between 70 and 240 nm and increased slightly with the increase of molar ratio of the additional water to TEOS. These results can be ascribed to that the incorporation of additional water can accelerate the hydrolysis reaction of TEOS, thereby the silica

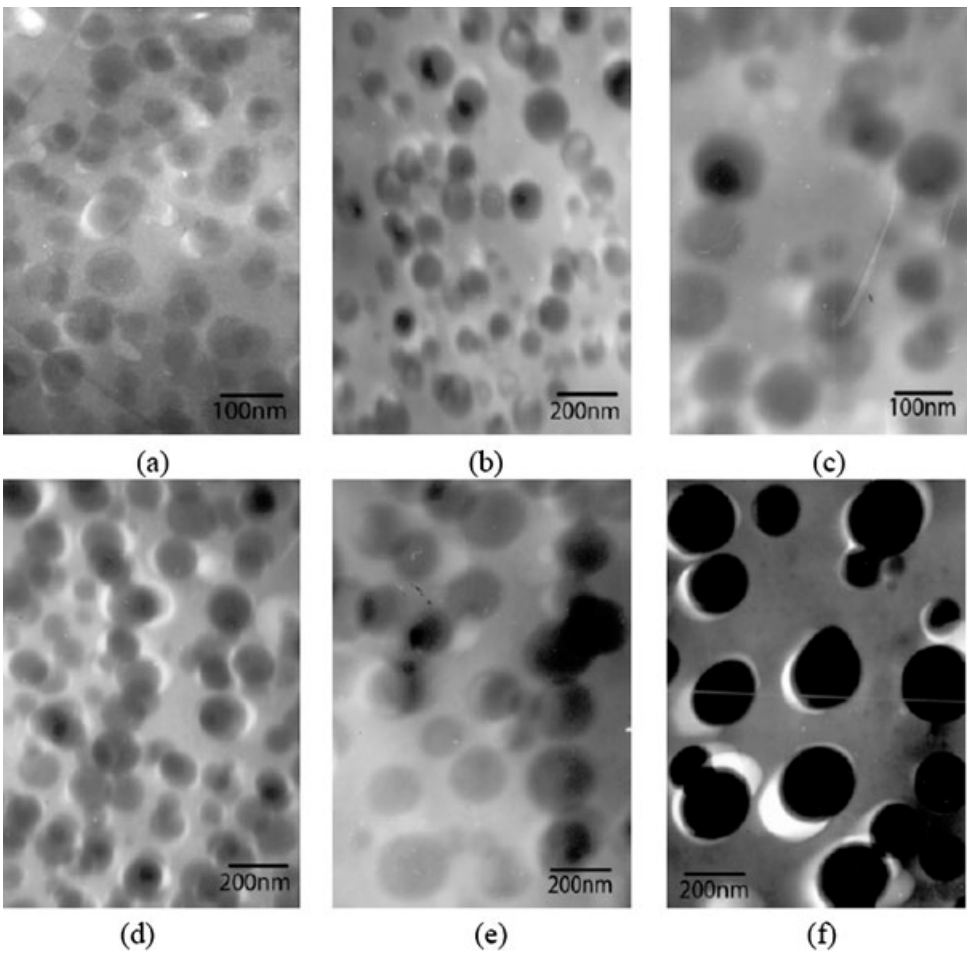

Figure 7 TEM images of the PI/SiO_2 nanocomposites with 10 wt % silica content prepared by (a) nonaqueous process, and at different molar ratio of additional water to TEOS: (b) 1 : 1, (c) 2 : 1, (d) 4 : 1, (e) 8 : 1, (f) 16 : 1.

particles from condensation reaction can aggregate easily in the early stage of PAA imidization to PI. The higher the molar ratio of additional water to TEOS, the easier the aggregation. As a result, the size of silica particles increases. When there is no additional water added during the sol–gel process, the hydrolysis reaction of TEOS might be initiated by the trace water yielded in the cycloimidization of PAA, which is a mode of self-catalyzed hydrolysis reaction.

The TEM images of nanocomposites prepared with and without additional water at different temperatures are shown in Figures 8 and 9, respectively. Figures 8(a) and 9(a) showed the TEM photos of two kinds of nanocomposite films before imidization. Comparing the images in Figure 8(a) with those in Figure 9(a), it can be seen that the silica particles formed in the PI matrix prepared under the condition of additional water, on the other hand, however, no silica particle was observed in the film prepared under the nonaqueous process. Figure 9(a,b) reveal that the silica particles were generated after the imidization reaction start. These results are in agreement with the results confirmed by the FTIR studies.

The mean size of silica particles assessed from the TEM photos are shown in Table I. The particle size increases with the increasing temperature up to 160°C. However, the particle size does not change after the temperature was increased to 300°C. The aggregation of silica particles in the nanocomposite films is influenced by the rigidity of matrix molecule chains; at the early stage of the imidization process, because the of the lower imidization degree and more flexible molecule chains, the particles can aggregate readily together to form larger particles. When the imidization is to be completed, the particles were hindered by the molecule network, and the particle size does not change again. The self-catalysis mechanism of the sol–gel reaction provides a relatively fast hydrolysis and a slow condensation reaction. As shown in Figure 1, the slow condensation reaction implies slow formation of the silica network, therefore providing a favorable condition for PI chains being able to penetrate into the silica network. Therefore, the PI/SiO_2 nanocomposites prepared from the above mechanism would thus lead to smaller silica particle sizes, and consequently, bring about some benefits in

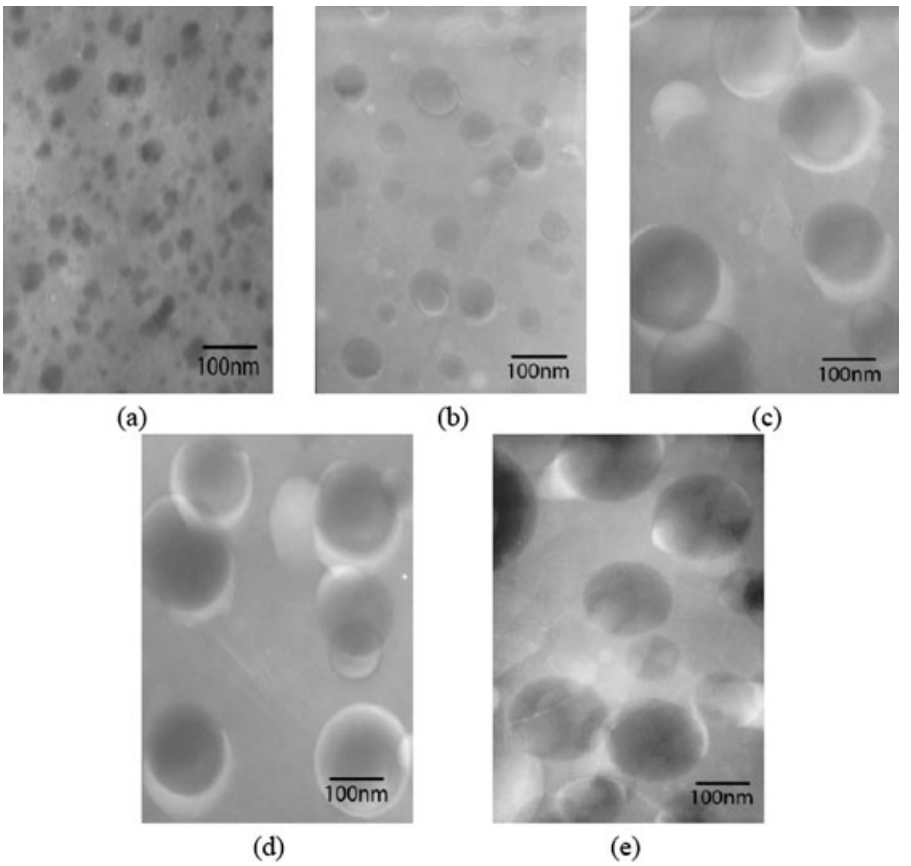

Figure 8 TEM images of the nanocomposite film with 10 wt % silica content via sol–gel with additional water (molar ratio of additional water to TEOS is 4:1) at temperatures of: (a) 20°C, (b) 80°C, (c) 120°C, (d) 160°C, (e) 300°C.

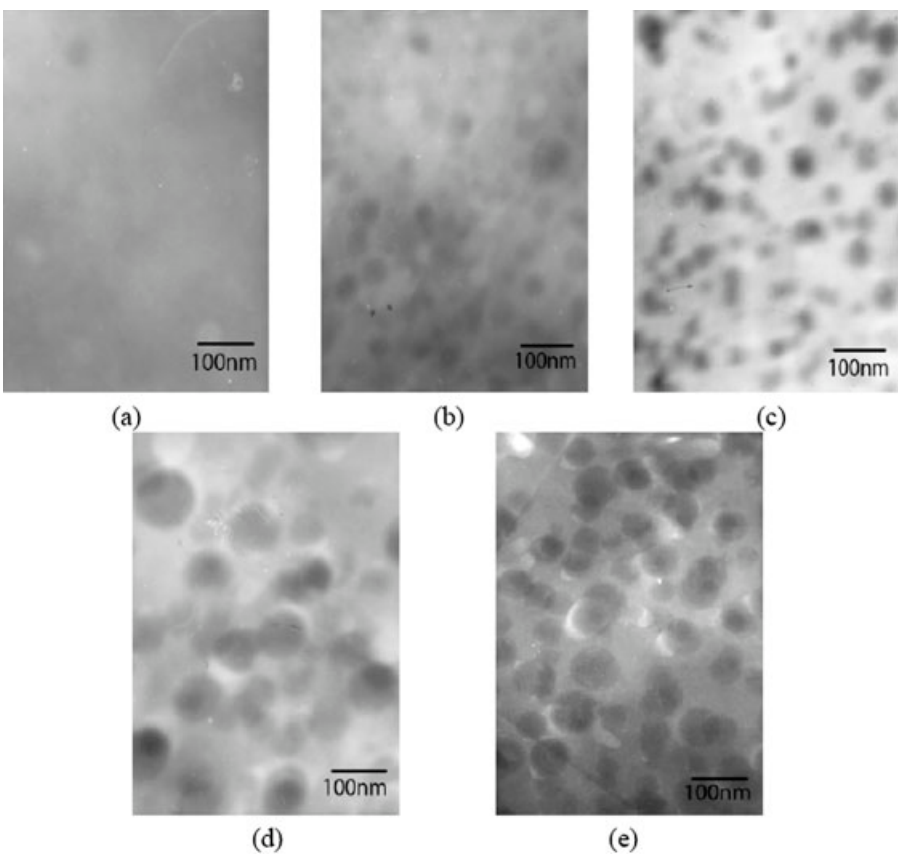

Figure 9 TEM images of the nanocomposite film with 10 wt % silica content via sol–gel process without additional water at temperatures of: (a) 20°C, (b) 80°C, (c) 120°C, (d) 160°C, (e) 300°C.

TABLE I
Size of SiO_2 Particles in the PI/SiO_2 Nanocomposite Films at Different Temperatures

	Size (nm)	
Temperature (°C)	With additional water (water to TEOS ratio : 4)	Without additional water
20	~25	No particles
80	~60	~30
120	~110	~50
160	~150	~70
300	~150	~70

improving the physical and mechanical properties of the PI/SiO_2 nanocomposite films.

Thermal and mechanical properties of the PI/SiO_2 nanocomposite films

The decomposition temperatures (5% weight loss) and char yield of the PI/SiO2 nanocomposites determined by TGA are listed in Table II. It can be observed from Table II that the decomposition temperatures of the nanocomposite decrease with the molar ratio of additional water to TEOS increase and all of those filled compound char yields are really the same. Firstly, at same silica content, the number of silica particles acting as crosslink point in the nanocomposite film decreases with the size of the silica particles increases, as shown in the TEM photos of the PI/SiO_2 nanocomposite films in Figure 7. Secondly, the incorporation of additional water may induce the hydrolysis of the PAA, and thus decrease of the molecular weight of the PAA and the so formed PI.

The tensile properties of the PI/SiO_2 nanocomposite films were also studied by Instron mechanical testing machine. The dependence of the tensile strength, elongation at break and tensile modulus of the films on the molar ratio of additional water to TEOS, and typical stress–strain curves of some nanocomposite films are shown in Figure 10. The PI/SiO_2 nanocomposite films prepared by sol–gel process without water addition have tensile strength of about 130 MPa, elastic modulus of 2.25 GPa and elongation at 22%. This tensile strength and elongation are much higher than that obtained under the conditions with

TABLE II
Decomposition Temperatures and Char Yield of PI/SiO_2 Nanocomposites with 10 wt % Silica Content at Different Molar Ratios of Additional Water to TEOS

Molar ratio of additional water to TEOS	Temperature at 5% weight loss ($T_{5\%}$) (°C)	Char yield at 800°C (%)
Unfilled PI	535	53.7
0 : 1	567	58.2
1 : 1	560.9	57.9
2 : 1	558.3	58.2
4 : 1	551.4	57.8
8 : 1	546.6	58
16 : 1	541.3	57.7

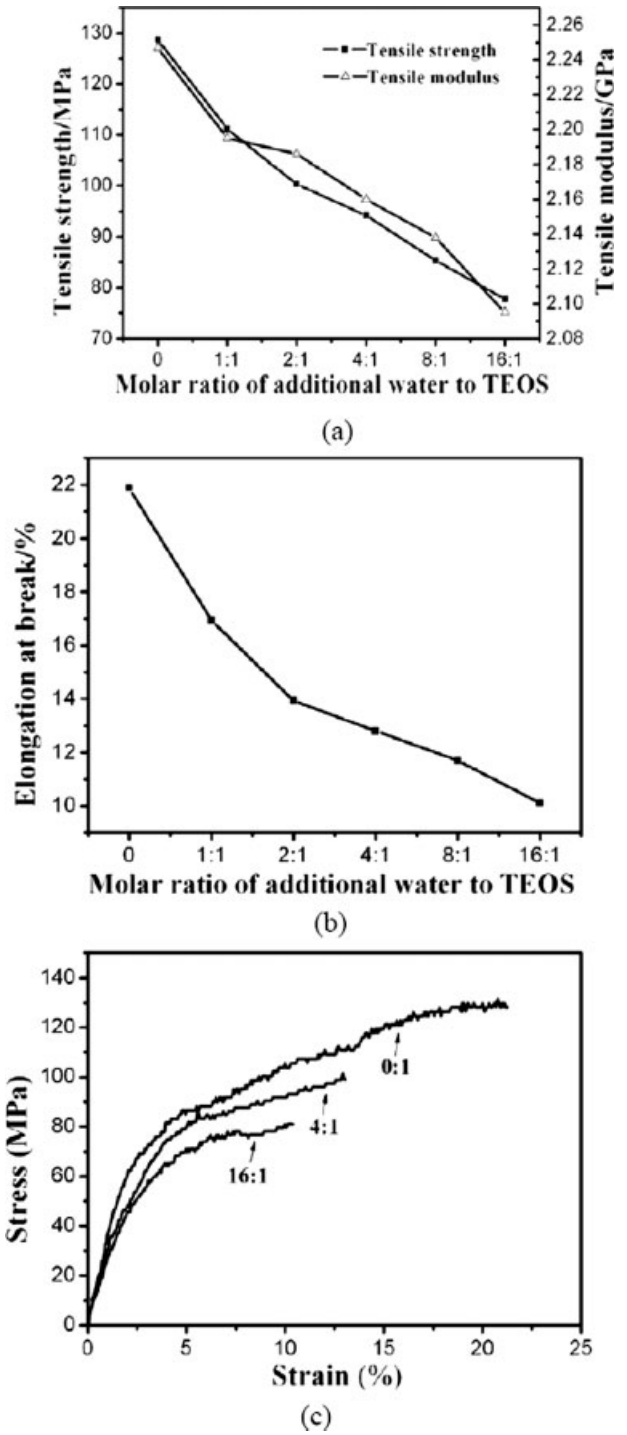

Figure 10 Effect of molar ratio of additional water to TEOS on the tensile properties of the PI/SiO_2 nanocomposite films with silica content of 10 wt %: (a) tensile strength, tensile modulus, (b) elongation at break, and (c) stress–strain curves.

additional water, as shown in Figure 10. It can also be seen from Figure 10 that with the increase in the molar ratio of additional water to TEOS, the PI/SiO_2 nanocomposite films become brittle and the mechanical properties (tensile strength, elongation at break, tensile modulus) of films decrease. Just as shown in Figure 1, water directly takes part in the formation of silica particles: when the additional water is low, the Si—OH group formed by hydrolysis reaction is few, so the silica nanoparticles formed from the condensation reaction of Si—OH group is smaller; on the contrary, when the additional water is high, the silica nanoparticles is bigger. The decrease in mechanical properties of the PI/SiO_2 nanocomposite films prepared with additional water can be attributable to the aggregation of silica particles. As well known, the aggregation of the silica particles lowered the nanoeffect of silica and aggravated the stress concentration. The existence of water might also induce the hydrolysis of PAA, reducing the molecular weight of the PAA and the following formed PI. As a result, the mechanical properties of the PI/SiO_2 nanocomposite films were deteriorated.

CONCLUSIONS

The effect of water on the preparation, structure, and properties of PI/SiO_2 nanocomposites by sol–gel process were investigated. At the same silica content, the additional water has been proved to be an adverse effect on preventing phase separation between PI and silica. By adjusting the molar ratio of water to TEOS, the size and distribution of silica particles in PI matrix can be controlled, and the properties of the PI/SiO_2 nanocomposite films can be improved effectively.

In the sol–gel process with additional water, the silica particles were generated before imidization and the particle size increased with the proceeding imidization process. In the sol–gel process without additional water, the silica particles *in situ* generated with the imidization reaction occurring, and the particle size increased with the proceeding imidization. In both of the process, the aggregation of silica particles was restricted by the rigidity of matrix molecule chains. Based on these studies, a new approach called *in situ* synchronization sol–gel process for preparing the PI/SiO_2 nanocomposites with the silica particles at nanometer scale was established. The PI/SiO_2 nanocomposites prepared from this approach lead to smaller silica particle sizes distributed in the PI matrix, and consequently improved physical and mechanical properties of the PI/SiO_2 nanocomposite films.

References

1. Novak, B. M.; Auerbach, D.; Verrier, C. Chem Mater 1994, 6, 282.
2. Landry, C. J. T.; Coltrain, B. K.; Wesson, J. A.; Zumbulyadis, N.; Lippert, J. L. Polymer 1992, 33, 1496.
3. Huang, H. H.; Wilkes, G. L.; Carlson, J. G. Polymer 1989, 30, 2001.
4. Wang, S.; Ahmad, Z.; Mark, J. E. Chem Mater 1994, 6, 943.
5. Jenekhe, S. A.; Osaheni, J. A. Chem Mater 1994, 6, 1906.
6. Chen, Y.; Iroh, J. O. Chem Mater 1999, 11, 1218.
7. Stefanithis, I. D.; Mauritz, K. A. Macromolecules 1990, 23, 2397.
8. Zhang, J.; Zhu, B. K.; Chu, H. J.; Xu, Y. Y. J Appl Polym Sci 2005, 97, 20.
9. Shao, P. L.; Mauritz, K. A.; Moore, R. B. Chem Mater 1995, 7, 192.
10. Zhong, S. H.; Li, C. F.; Xiao, X. F. J Membr Sci 2002, 199, 53.
11. Chang, C. C.; Chen, W. C. Chem Mater 2002, 14, 4242.
12. Musto, P.; Ragosta, G.; Scarinzi, G.; Mascia, L. Polymer 2004, 45, 4265.
13. Cornelius, C. J.; Marand, E. Polymer 2002, 43, 2385.
14. Hibshman, C.; Cornelius, C. J.; Marand, E. J Membr Sci 2003, 211, 25.
15. Chen, B. K.; Chiu, T. M.; Tsay, S. Y. J Appl Polym Sci 2004, 94, 382.
16. Morikawa, A.; Yamaguchi, H.; Iyoku, Y. J Mater Chem 1992, 2, 679.
17. Jiang, L. Z.; Feng, Y. Z.; Wu, D. Z. J Beijng Univ Chem Technol 2005, 32, 59.
18. Iyoku, Y.; Kakimoto, M.; Imai, Y. High Perform Polym 1994, 6, 43.
19. Mascia, L.; Kioul, A. Polymer 1995, 36, 3649.
20. Schrotter, J. C.; Smaihi, M.; Guizard, C. J Appl Polym Sci 1996, 61, 2137.
21. Wang, H.; Zhong, W.; Xu, P.; Du, Q. Macromol Mater Eng 2004, 289, 793.
22. Hsiue, G. H.; Chen, J. K.; Liu, Y. L. J Appl Polym Sci 2000, 76, 1609.
23. Musto, P.; Ragosta, G.; Scarinzi, G.; Mascia, L. Polymer 2004, 45, 1697.
24. Zhu, Z. K.; Yang, Y.; Yin, J.; Qi, Z. N. J Appl Polym Sci 1999, 73, 2977.